Chapter 3

Thermally-Induced Phase Separation Mechanism Study for Membrane Formation

Sung Soo Kim, Min-Oh Yeom, and In-Sok Cho

Department of Chemical Engineering, Institute of Material Science and Technology, Kyung Hee University, Yongin City, Kyunggido 449–701, Korea

The thermally-induced phase separation mechanism was investigated for the system isotactic polypropylene and diphenyl ether. Droplet growth was monitored by using a thermo-optical microscope. The degree of supercooling for liquid-liquid phase separation affected the size and growth rate of the droplets. Increasing the polymer content affected the solution viscosity and interaction parameter which resulted in a decrease of the size and growth rate of the droplets. Crystallization interfered with the droplet growth at lower quench temperatures from the onset of crystallization. The droplet growth rate followed the equation proposed by Furukawa, and the droplet growth was well described by the theories for coarsening and coalescence. Equilibrium droplet size was estimated by the Laplace equation and was in good agreement with the experimental data. The cell size of the membrane was about half of the droplet size of the melt sample due to shrinkage of the sample during extraction of the diluent and the drying process.

Development of semicrystalline polymer membranes is important for many membrane processes because they can withstand high-temperature operating conditions and are resistant to aggressive chemicals (*1*). Moreover, microporous semicrystalline polymer membranes can be used in other applications such as battery separators (*2*). The thermally-induced phase separation (TIPS) process is one of the most promising fabrication methods of making microporous semicrystalline membranes (*3*). Controlling the structure of the membrane made via TIPS requires an understanding of the phase separation mechanisms. Specifically, the liquid-liquid phase separation process induced by the thermodynamic instability

of the system must be examined in detail for the interpretation of the microcellular structure formation (*4*).

As shown in Figure 1, when the homogeneous melt solution (D) enters the liquid-liquid phase separation region (C), it undergoes spinodal decomposition to form a polymer-rich (R) and a polymer-lean (L) phase (*5,6*). If the sample is held at T, the phase-separated domain (liquid droplet) grows via a coarsening process followed by coalescence of the droplets to form an even greater droplet (*7-9*). The sample is then quenched in ice water to induce crystallization of the polymer, which freezes the structure. Following extraction of the diluent, a microcellular structure is obtained (*10,11*).

In this work, the system isotactic polypropylene (PP) and diphenyl ether (DPE) was investigated for membrane fabrication via TIPS. The PP/DPE system forms a homogeneous melt solution above the melting temperature of the mixture and undergoes liquid-liquid or solid-liquid phase separation depending on the initial polymer concentration. Several factors affecting the phase separation mechanisms were examined, that is, (i) phase separation temperature, (ii) crystallization temperature, and (iii) initial composition of the melt solution. Droplet formation and growth were monitored for interpretation of the phase separation mechanism. The droplet growth kinetics were analyzed and compared with the results of McGuire and Laxminarayan who also studied the TIPS process for the PP/DPE system (*12-15*). The interfacial tension between the phase-separated domains was determined to estimate the equilibrium domain size. The cell size of the membrane was compared with the droplet size of the melt solution to study the droplet growth behavior to the real cell growth behavior.

Experimental

Isotactic PP (H730F) was supplied by SK Co., Korea, and DPE was obtained from Aldrich Co. PP is one of the most preferred materials in this application, because it has advantages over other materials in terms of processability, thermal and chemical resistance, and price. DPE was selected as a diluent in this work, because it forms a homogeneous melt solution with PP at high temperature, which undergoes liquid-liquid phase separation by lowering the temperature. The refractive index of DPE (n_D^{20}=1.579) is different from that of PP (n_D^{20}=1.490), which enabled us to observe the sharp interfaces between the polymer-lean and polymer–rich phases formed by the liquid-liquid phase separation process via optical microscopy. Methanol (Aldrich Co.) was used to extract the DPE after phase separation was completed. PP and DPE were melt blended at 210°C to make homogeneous melt solutions. The sample was quenched into ice water to form solid samples.

Perkin Elmer DSC 7 was used for the thermal analyses of the samples and a Hitachi S-4200 scanning electron microscope (SEM) was used to examine the structure of the membranes. A thermo-optical microscope (TOM) system was assembled as shown in Figure 2, which consisted of a Zeiss Jenaval microscope, a

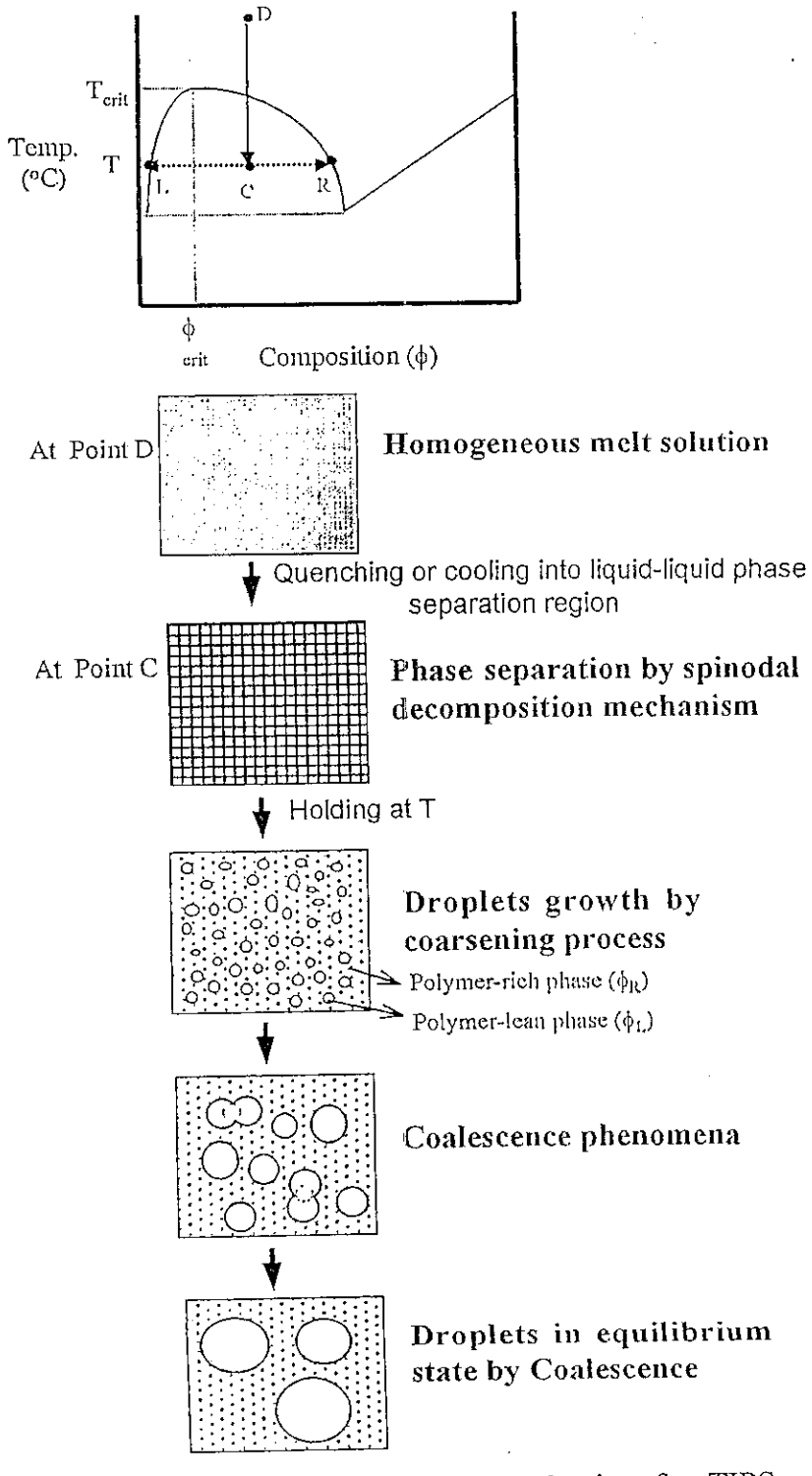

Figure 1. Liquid-liquid phase separation mechanism for TIPS membrane formation.

Mettler hot-stage (FP-82) with central processor (FP-90), and an image analyzer system (IP lab) equipped with CCD camera, VCR, and video printer. The Laplace equation was used to estimate the equilibrium droplet size. In order to determine the interfacial tension, the surface tensions of the melt solution and diluent were measured by using a modified TOM system, as shown in Figure 3. Each shape of the drop was captured for the calculation of the surface tension by using the pendant drop method proposed by Andreas *et al.* (*16*).

Results and Discussion

The phase diagram of the PP/DPE system was determined experimentally, as shown in Figure 4. Cloud points were determined using the TOM system, and the melting temperatures (T_m) and crystallization temperatures (T_c) were obtained by DSC at a scanning rate of 10°C/min. The melt-blended samples were held at 210°C for 10 min to eliminate the thermal history of the sample before scanning. Figure 4 shows a typical phase diagram for a liquid-liquid phase separation system of a semicrystalline polymer, whose monotectic point, the intersection point of the cloud point curve and crystallization curve, is located at 94°C and 40 wt.% PP at a 10°C/min cooling rate. McGuire *et al.* also generated a phase diagram for the same system which showed similar cloud points as reported here (*12*). However, McGuire *et al.* determined the equilibrium melting temperature, which is much higher than the dynamic T_m and T_c determined in this work. Therefore, the location of the monotectic points should be different from each other due to the different scanning rates. The location of the sample relative to the equilibrium melting temperature in the phase diagram had great influence on the crystallization of PP. When the PP content was lowered to less than 10 wt.%, the sample had poor integrity and could not be used for the determination of the phase diagram.

A homogeneous melt solution of a 10 wt.% PP/90 wt.% DPE sample at 210°C was placed onto the hot-stage preset at 110°C. Placing the 210°C sample on the hot-stage at 110°C made the hot-stage temporarily unstable and it took about 3 seconds for the sample and the hot-stage to reach equilibrium. It was difficult to quantify the cooling rate for this quenching step. The sample was prepared between the cover slips and the edges were sealed with silicon sealant. There was little diluent loss during the experiment, and the weight change before and after the test was less than 3% of the initial weight. The phase separation images at 110°C were captured at different times, as shown in Figure 5. The number labeled in each picture represents the elapsed time after the hot-stage reached equilibrium in hr:min:sec mode. Images of phase separation by spinodal decomposition were observed immediately; however, the onset of spinodal decomposition could not be observed. After 5 minutes, phase-separated droplet growth via coarsening was observed in the optical microscope. The droplets continued to grow until 1 hr and 30 min. In its later stages of liquid-liquid phase separation, coalescence of droplets

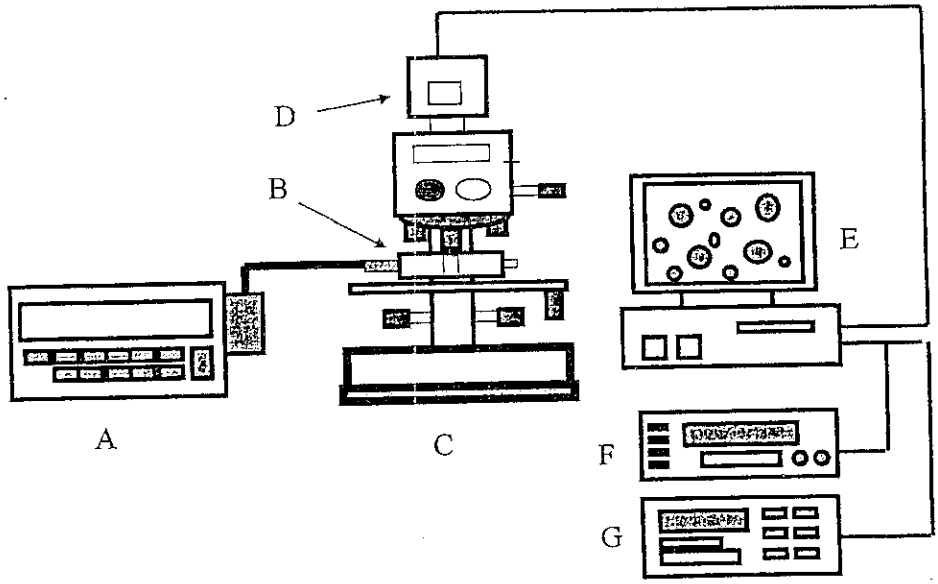

Figure 2 A schematic diagram of a thermo-optical microscope system. A: central processor, B: hot-stage, C: optical microscope, D: CCD camera E: image analyzer system, F: VCR, G: video printer.

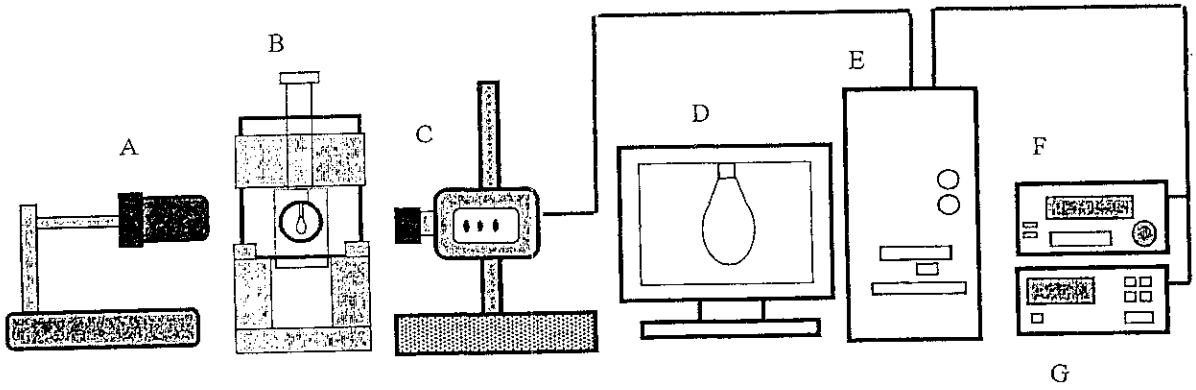

Figure 3. A schematic diagram of a surface tension measurement system. A: light source, B: pendant drop assembly, C: CCD camera, D: monitor, E: image analyzer system, F: VCR, G: video printer.

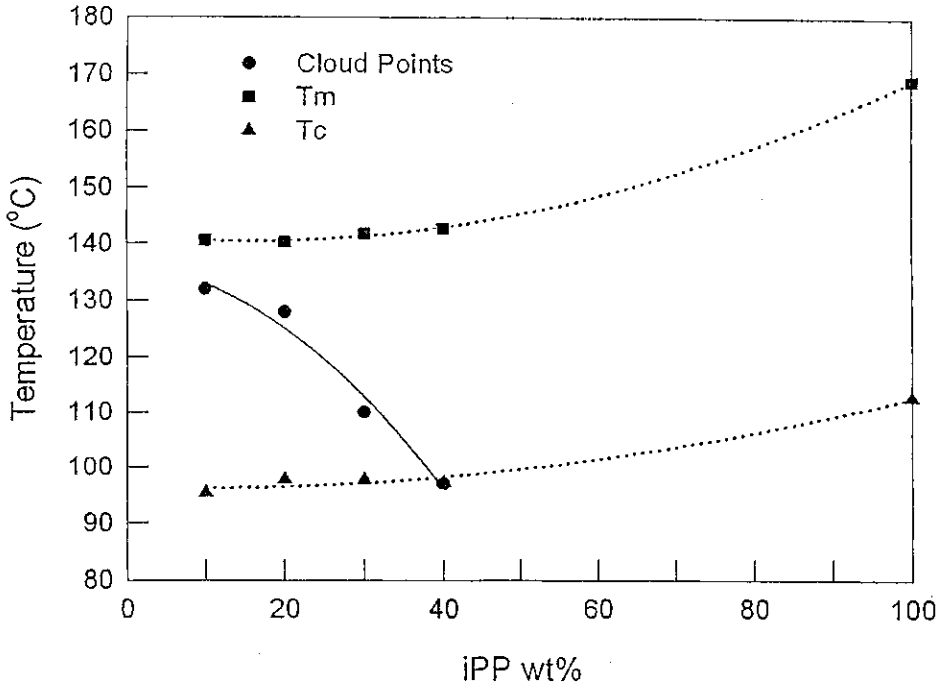

Figure 4. Phase diagram of the PP/DPE system determined at 10°C/min.

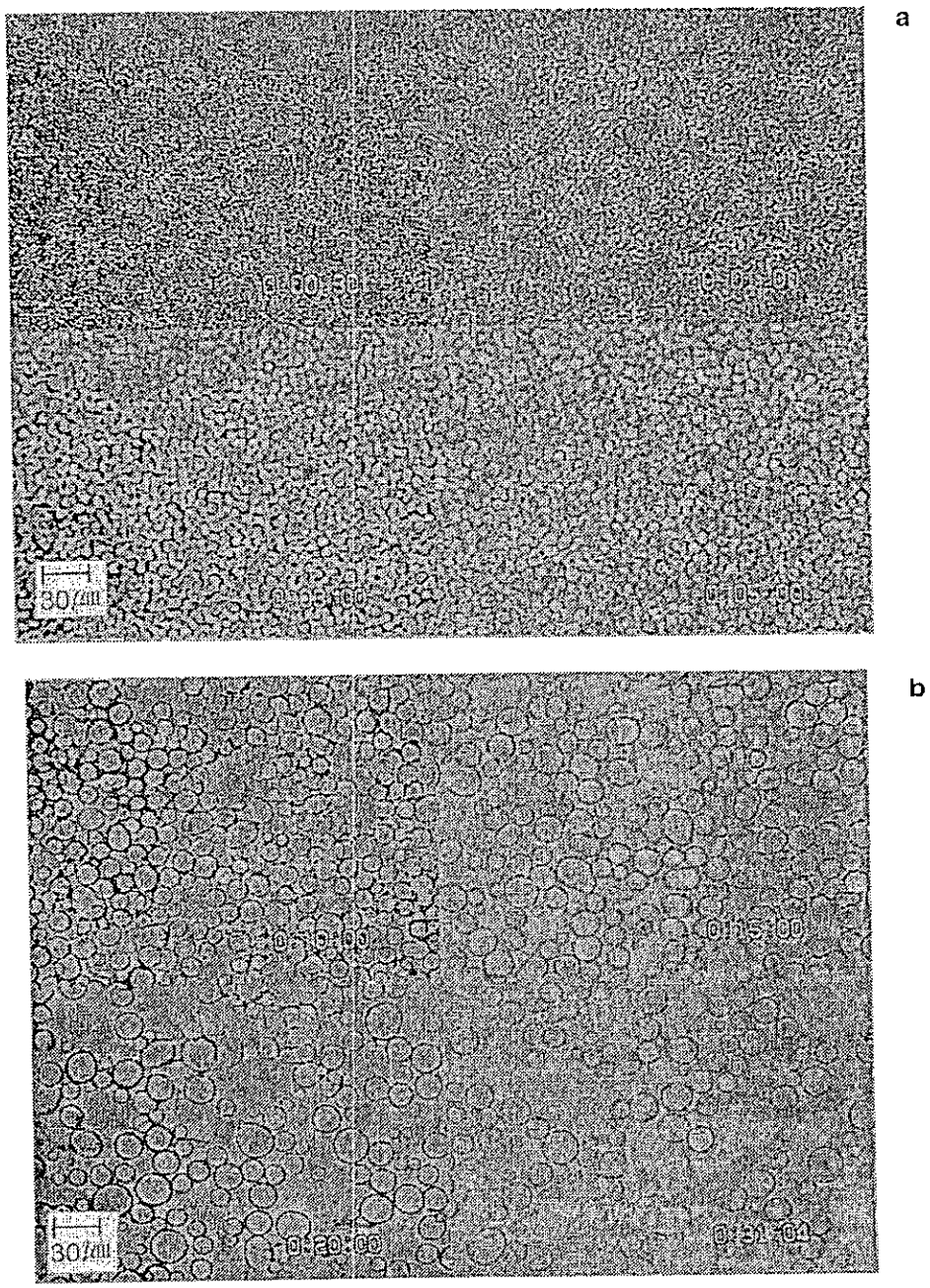

Figure 5. Images of phase separation for PP/DPE = 10/90 wt.% at 110°C (numbers in each image represents hr:min:sec).

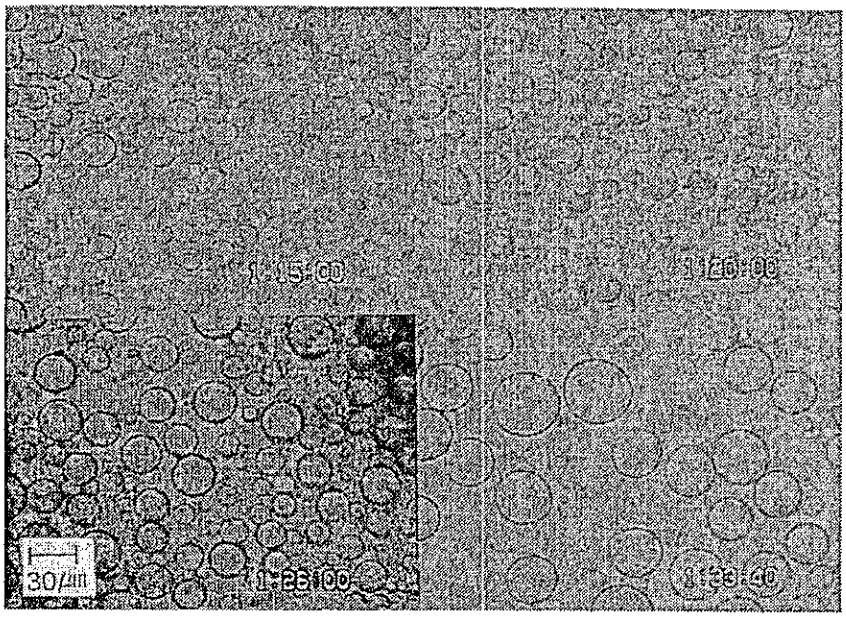

C

Figure 5. *Continued.*

was observed, as shown in the upper left corner of Figure 6. Coalescence of droplets resulted in large cells after extraction of the diluent.

Similar observations were obtained for other samples with different compositions and at other quench temperatures. Each droplet size was obtained by averaging the sizes of 50 to 60 droplets, and each experiment was repeated three times to ensure the reproducibility of the data. Temperature dependence of the droplet growth was examined in more detail by selecting various quench temperatures from 105°C to 125°C. The temperature dependence of the growth rate is shown in Figures 7 and 8. Our results are similar to those of McGuire *et al.* (*12*). The growth rate and the size of the droplets increased as the quench temperature was lowered. A decrease in quench temperature caused a greater supercooling for liquid-liquid phase separation, which is defined as the temperature difference between the cloud point temperature and the quench temperature. Greater supercooling changed the viscosity of the matrix and the droplet phases, the volume fractions of the two phases, and the interfacial tension. Therefore, increased supercooling accelerated the droplet growth (*17-19*) and the size and growth rate of the droplets increased as the holding temperature was lowered for the 10 and 20 wt.% PP samples.

At lower temperature PP crystallization interfered with the droplet growth. Although the holding temperature was located above the dynamic crystallization curve at a scanning rate of 10°C/min, it is located under the equilibrium melting temperature reported by McGuire *et al.* (*12*). Consequently, there was a thermodynamic driving force for crystallization (*20,21*). The degree of supercooling for crystallization is defined as the temperature difference between the equilibrium melting temperature and the holding temperature. Greater supercooling also accelerated crystallization, and there was no more droplet growth after a certain degree of crystallization, because the crystallization process froze the structure.

The dependence of droplet growth on composition was also explored for phase separation temperatures of 115 and 125°C, as shown in Figures 9 and 10, respectively. The droplet growth behavior depended strongly on the composition. Both the growth rate and the size of the droplet decreased with an increase of PP content at each quench temperature. An increase of polymer concentration increased the solution viscosity, which limited the droplet growth. The interaction parameter between PP and DPE depended on the composition and it also had influence on the droplet growth (*22*). With an increase in polymer concentration the nucleation density for crystallization increased (*20,21*). For a 20 wt.% PP sample the droplet growth was suspended at 20 min (115°C) and 40 min (125°C) by the interference of PP crystallization. Crystallization of PP at 105°C began at 6 minutes and it interfered with the droplet growth beyond this point, as shown in Figure 11. The droplet could not reach the equilibrium size, when the PP composition was high and the crystallization temperature was low.

In order to estimate the equilibrium droplet size we used the Laplace equation

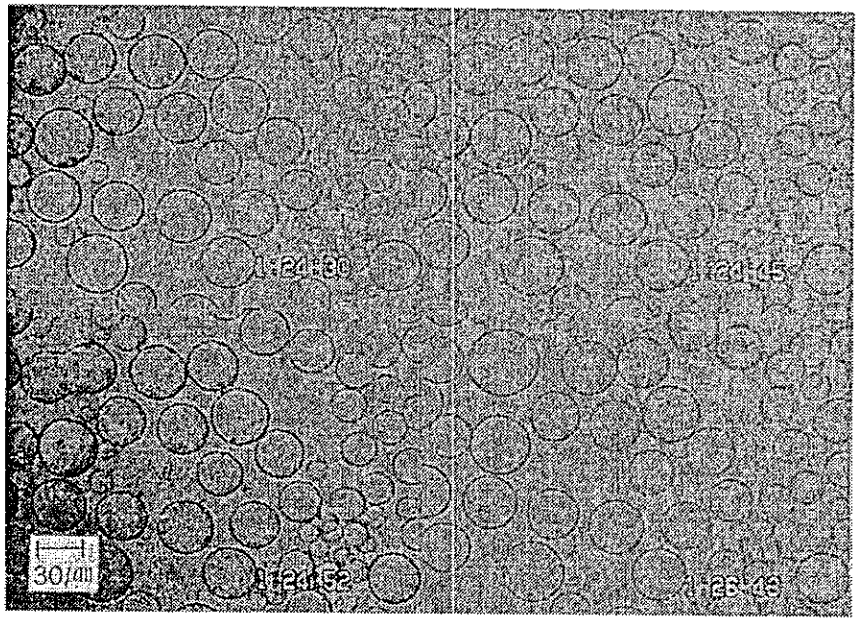

Figure 6. Coalescence images at the later stage of phase separation.

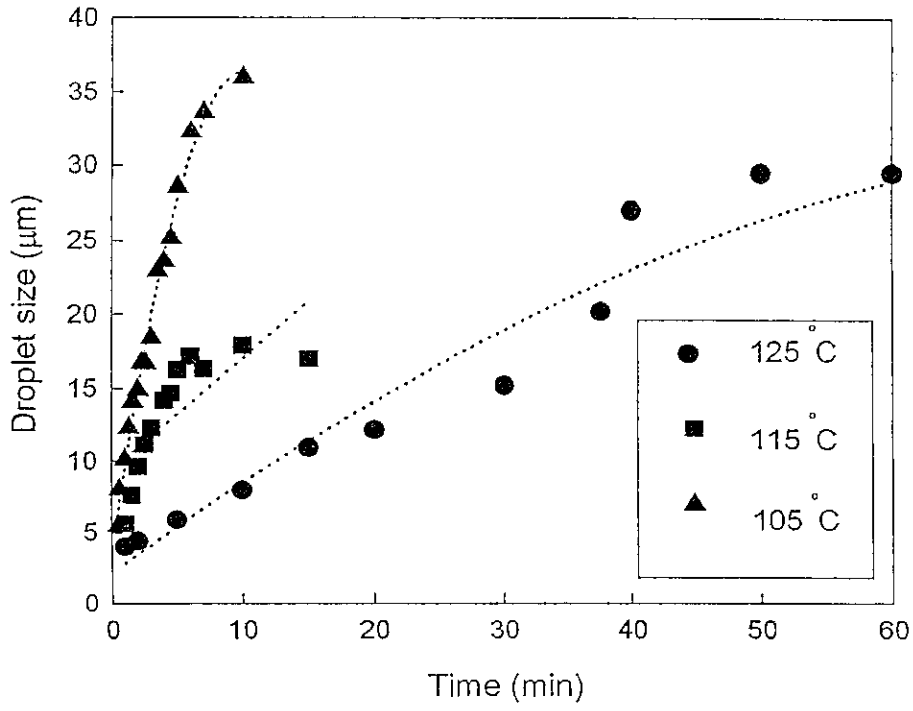

Figure 7. Droplet growth at different phase separation temperatures for PP/DPE=10/90 wt.%.

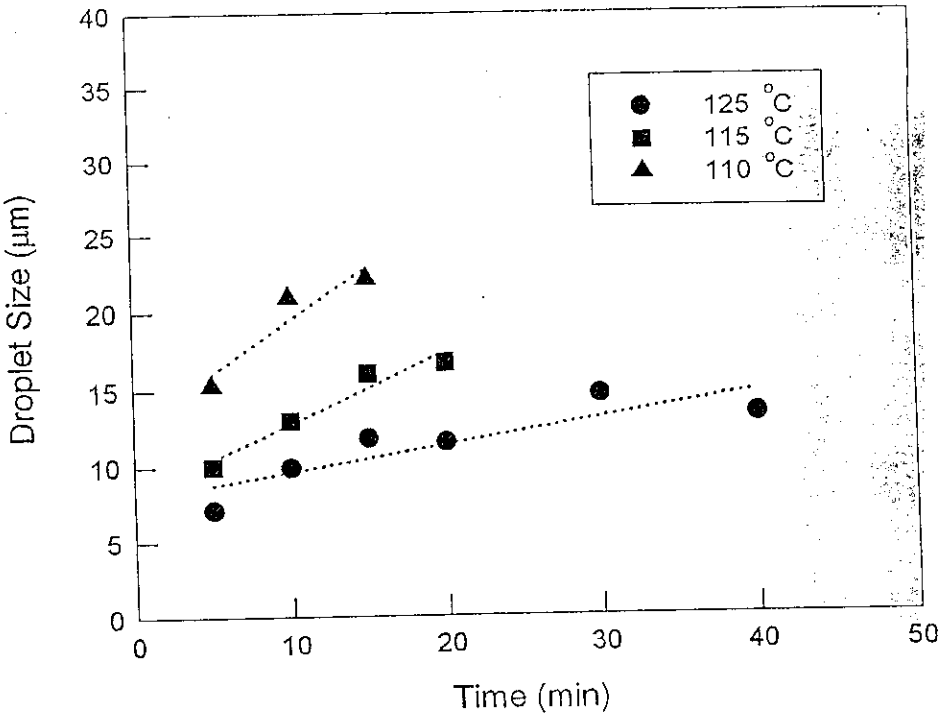

Figure 8. Droplet growth at different phase separation temperatures for PP/DPE=20/80 wt.%.

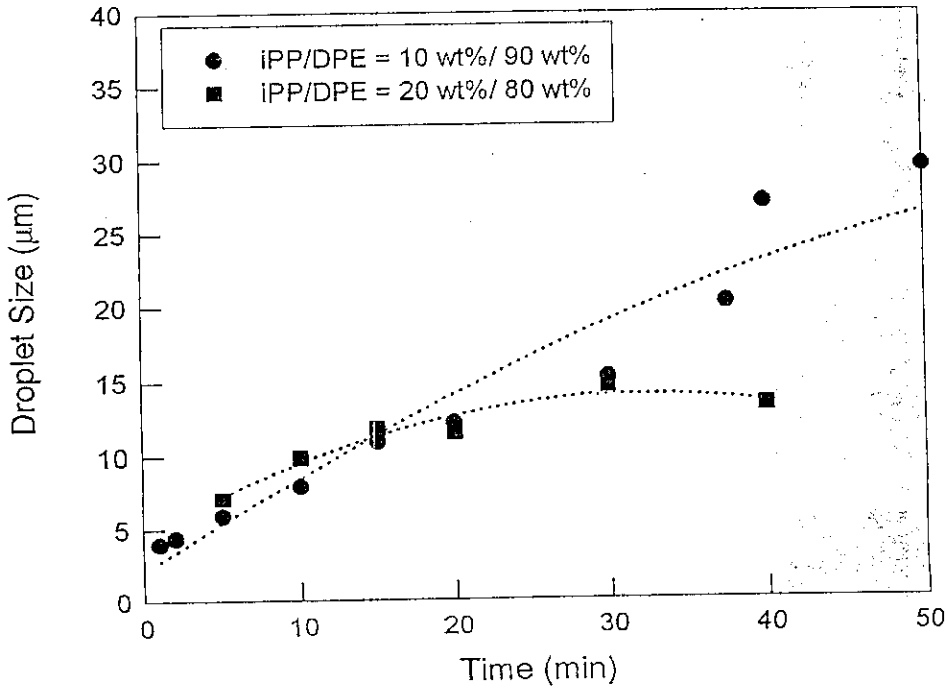

Figure 9. Droplet growth for different PP/DPE compositions at 115°C.

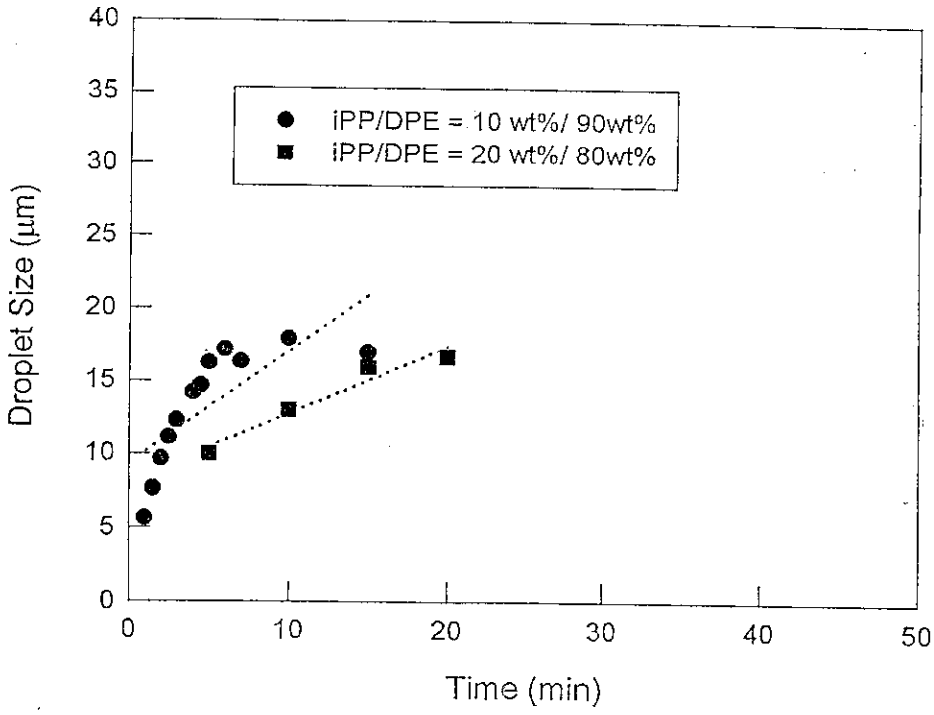

Figure 10. Droplet growth for different PP/DPE compositions at 125°C.

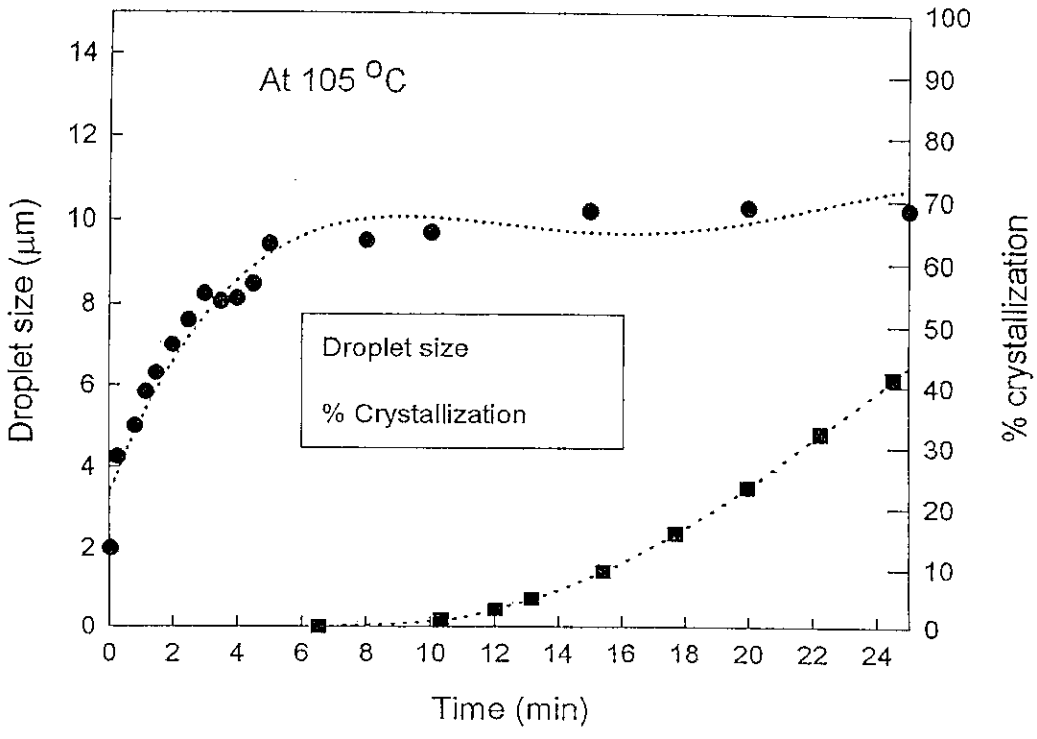

Figure 11. Droplet growth and crystallization at 105°C for PP/DPE=20/80 wt.%.

for a spherical drop:

$$r = 2\gamma / \Delta p \quad (1)$$

where r is the radius of the droplet, Δp is the pressure difference, and γ is the interfacial tension between the phases (*23*). In this work, we used the vapor pressure difference between the polymer-lean and polymer-rich phase for equation 1. The vapor pressure of the polymer was ignored and the polymer-lean phase was assumed to be composed of pure diluent. Therefore, the vapor pressure of the polymer lean-phase was equal to the vapor pressure of the diluent. The vapor pressure of the polymer-rich phase was estimated by the product of the vapor pressure of the diluent (*24*) and the diluent fraction.

The interfacial tension between the phases must be determined to estimate r by equation 1. It can be measured by several techniques such as the sessile drop, spinning drop, and pendant drop method (*16,23*). McGuire *et al.* determined the interfacial tension of the phases in the PP/DPE system by a spinning drop method (*12*). Previously, the pendant drop method was discussed by several authors (*23,25*). The method of Andreas defines a shape-dependent quantity S as:

$$S = d_s / d_e \quad (2)$$

where d_s is the equatorial diameter, and d_e is the diameter at a distance from the bottom of the drop as shown in Figure 12.
The parameters H and β are defined as:

$$H = -\beta (d_e / b)^2 \quad (3)$$

$$\beta = -(\Delta\rho\, g\, b^2) / \gamma \quad (4)$$

where b is the radius of the drop at the apex, $\Delta\rho$ is the density difference between the phases and g is the gravitational constant. Then the surface tension, γ, is expressed by equation 5.

$$\gamma = (\Delta\rho\ g\, d_e^{\,2}) / H \quad (5)$$

From the shape of the drop we measured d_e and d_s from which S was calculated. 1/H was obtained from Fordham's Table (*25*). Because the densities of polymer-rich and polymer-poor phase were similar, we could not form a pendant drop of the polymer-lean phase in the polymer-rich phase. Therefore, we could not directly measure the interfacial tension between the phases. However, for nonpolar compounds Fowke's relationship can be applied, which is expressed as

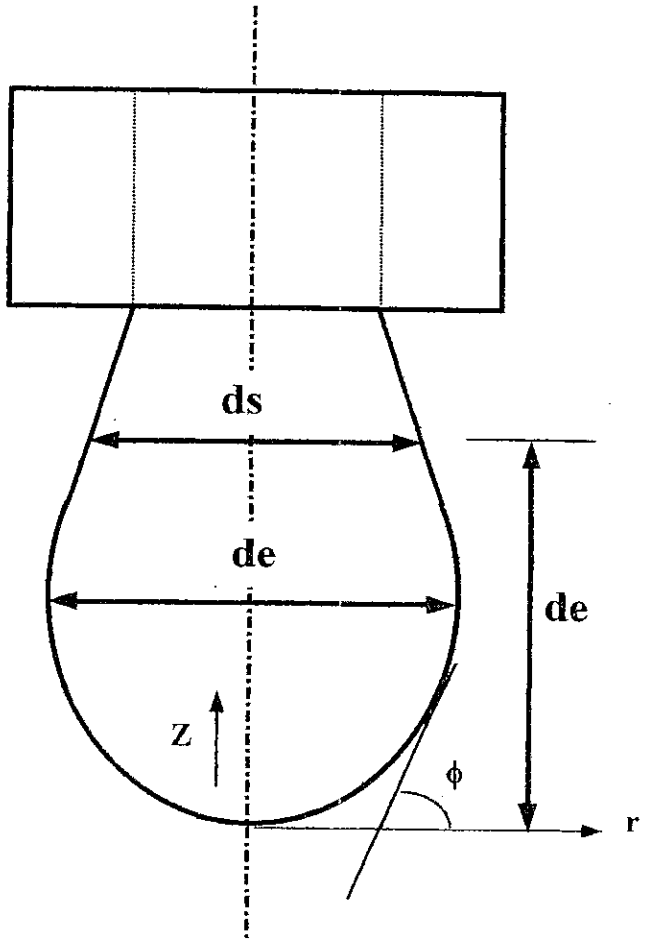

Figure 12. Geometry of the pendant drop in a selected plane.

$$\gamma_{12} = (\gamma_1^{1/2} - \gamma_2^{1/2})^2 \quad (6)$$

where γ_{12} is the interfacial tension between phases 1 and 2, and γ_1 and γ_2 are the surface tensions of phases 1 and 2, respectively (*26*).

The PP/DPE system phase separated into a polymer-lean phase (ϕ_p=0) and a polymer-rich phase (ϕ_p=0.2) at 125°C. We measured the surface tensions of pure diluent and the 20 wt.% PP sample at 125°C. The interfacial tension between the phases at 125°C was 0.59 dyne/cm, which was higher than that determined by McGuire *et al.* (*12*). The experimental data for obtaining the interfacial tension are summarized in Table I. With the interfacial tension value and the vapor pressure of the diluent (*24*), we estimated the equilibrium droplet size as 12.6 μm at 125°C, which is in good agreement with the experimental value of 13.3 μm.

Table I. Experimental data for estimation of the interfacial tension of polymer-lean phase and polymer-rich phase of the PP/DPE system at 125°C

Property	Polymer-rich phase (20 wt.% PP)	Polymer-lean phase (pure diluent)
Density (g/cm^3)	0.877	0.984
d_e	1.85	1.70
d_s	1.20	1.23
S	0.65	0.72
1/H	0.95	0.73
Surface tension(dyn/cm)	27.9	20.4
Interfacial tension (dyn/cm)	0.59	

Droplet growth kinetics studies were previously performed by several investigators. Lifshitz and Slyozov described the coarsening process using an asymptotic power law relating the domain size (d) with time (t) as follows:

$$d \sim (D\,\xi)^{1/3}\, t^{1/3} \quad (7)$$

where D is the diffusion coefficient and ξ is the correlation length (27,28).

When two droplets overlap and dissolve at their interface, a larger drop will be formed. This process is referred to as coalescence or collision-combination mechanism. In this case, the size of the dispersed phase (d) is expressed as,

$$d \sim [k_B T/\eta]^{1/3}\, t^{1/3} \quad (8)$$

where k_B is the Boltzmann constant, T is the phase separation temperature, η is the solution viscosity, and t is time (*29-31*).

In the bicontinuous phase after phase separation, the pressure gradient between the regions with different curvature causes the hydrodynamic flow to form larger droplets. In this case, the droplet diameter (d) can be expressed as a function of surface tension (σ), viscosity of the continuous phase (η), and time (t) (*7,28*):

$$d \sim (\sigma / \eta)\, t \tag{9}$$

Recently, Furukawa proposed a theory in which the single length scale was set as a function of time. This is a more general form of the coarsening process, and the length scale (d) is expressed as:

$$d = \kappa \cdot t^{\lambda} \tag{10}$$

where κ is a proportional constant and λ is a scaling exponent or growth exponent which is related to the microscopic particle growth (*32*). This mechanism can be applied to a phase-separated polymer solution system regardless of whether the system undergoes phase separation by spinodal decomposition or by nucleation and growth.

Furukawa's theory was applied to the systems studied in this work, and the results are shown in Table II.

Table II. Proportional constants and scaling exponents of Furukawa equation for PP/DPE systems at different composition and temperature.

(a) 10 wt.% PP/DPE

Quench temperature	125°C	115°C	105°C
Proportional constant (κ)	3.54	6.91	9.77
Scaling exponent (λ)	0.38	0.43	0.51

(b) 20 wt% PP/DPE

Quench temperature	125°C	115°C	110°C
Proportional constant (κ)	4.47	5.37	8.91
Scaling exponent (λ)	0.31	0.36	0.35

As the quench temperature decreased, κ increased, which indicates an increase of the droplet size and its growth rate. The scaling exponent, λ, increased as the PP

content decreased from 20 to 10 wt.%. For the 10 wt.% PP sample, λ increased as the quench temperature decreased. On the other hand, λ was essentially constant (~0.3) for the 20 wt.% PP sample independent of the quench temperature, as proposed by Furukawa (*32*). McGuire *et al.* also determined the λ value for the PP/DPE system, and showed a similar trend to our data. However, for the 20 wt.% PP sample we obtained a greater value of λ than McGuire (*12*).

Droplets formed during liquid-liquid phase separation consisted mainly of diluent and the sites occupied by the droplets formed cells after extraction of the diluent. Therefore, the cell size of the membrane was expected to be directly related to the droplet size. The samples on the hot-stage for the droplet growth observation were saved and the diluent was extracted. SEM images of the samples are shown in Figures 13 to 15. As the holding time of the 20 wt.% PP sample at 110°C increased, the cell size increased (Figure 13), which is the same trend for the droplet growth, as shown in Figures 7 to 10. However, there was not much difference between the 10 min and 30 min samples, because PP crystallization interfered with the droplet growth of the sample after 10 minutes.

The effect of quench temperature on the cell size was also examined, as shown in Figure 14. By lowering the holding temperature, the cell size increased as well as the droplet size. The cell size increased until the quench temperature reached 110°C. However, at 105°C the cell size decreased due to crystallization of the polymer, although it had the greatest supercooling for liquid-liquid phase separation of the samples. An increase of polymer concentration reduced the cell size, as shown in Figure 15.

From the images of droplets and SEM images of cells we can conclude that the cell size is directly related to the droplet size. The absolute size of the droplet and the cell of the same sample are compared in Figure 16. The cell size was about half of the droplet size. The smaller cell size resulted from shrinkage of the sample during extraction of the diluent and the subsequent drying process. Factors that determine the degree of shrinkage are: (i) the type of extractant, (ii) the polymer concentration of the sample, and (iii) the evaporation rate of the extractant. A more systematic study on the sample shrinkage is currently being performed and will be reported in a future paper.

Conclusions

As the degree of supercooling for liquid-liquid phase separation increased in the PP/DPE system, the size and growth rate of the droplets increased. However, the degree of supercooling for crystallization also increased and crystallization interfered with the droplet growth at a lower quench temperature. An increase of polymer concentration affected the solution viscosity and interaction parameter, which resulted in a decrease of the size and growth rate of the droplets. The

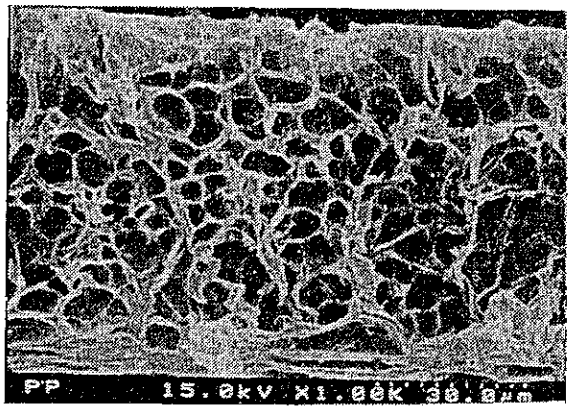

(a) holding time :1min

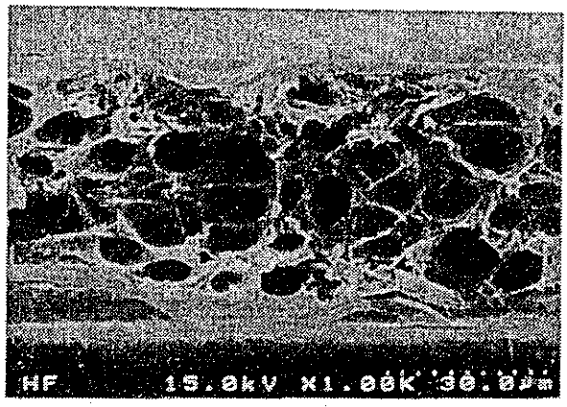

(c) holding time :10min

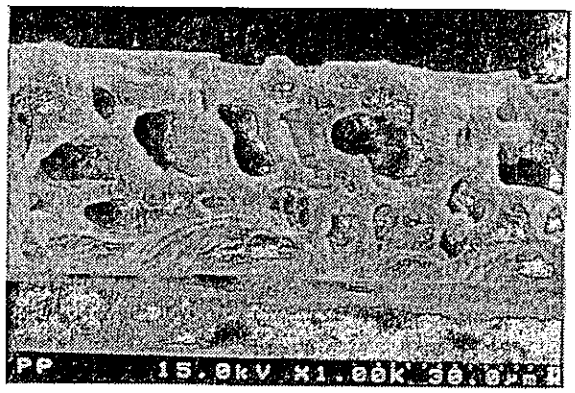

(b) holding time : 5min

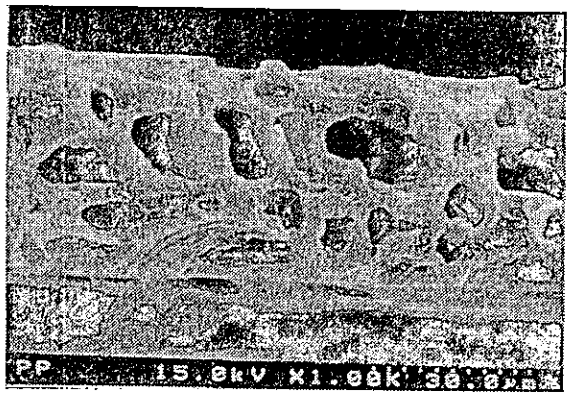

(d) holding time :30min

Figure 13. SEM images of membranes held at 110°C for different intervals (PP/DPE = 20/80 wt.%).

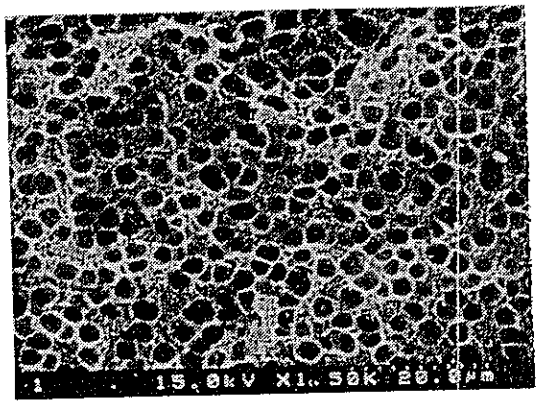

(a) 210 °C → 120 °C

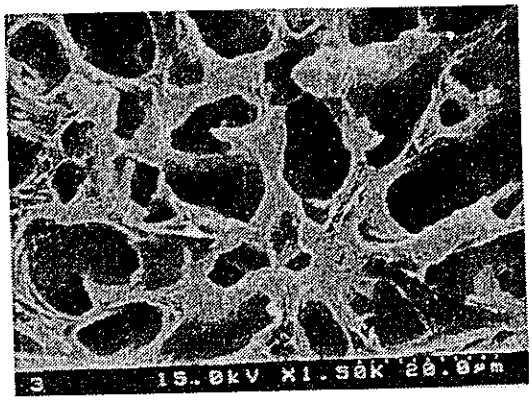

(c) 210 °C → 110 °C

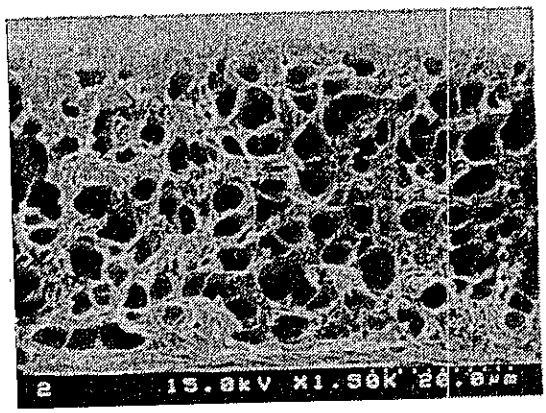

(b) 210 °C → 115 °C

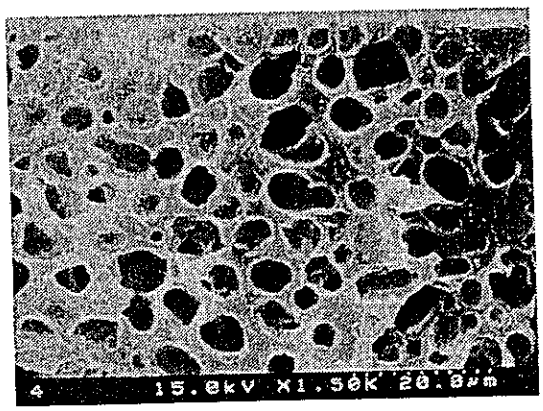

(d) 210 °C → 105 °C

Figure 14. SEM images of membranes held at different temperatures for 10 minutes (PP/DPE = 20/80 wt.%).

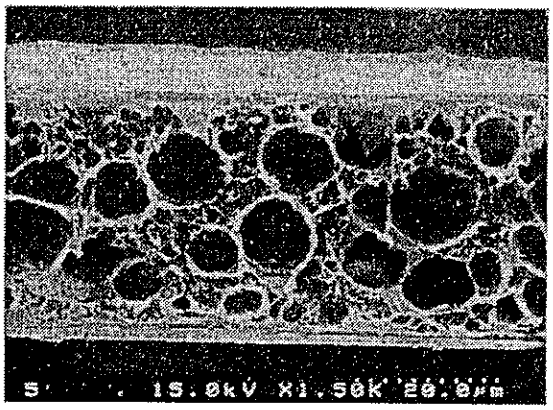

(a) 210 °C → 115 °C

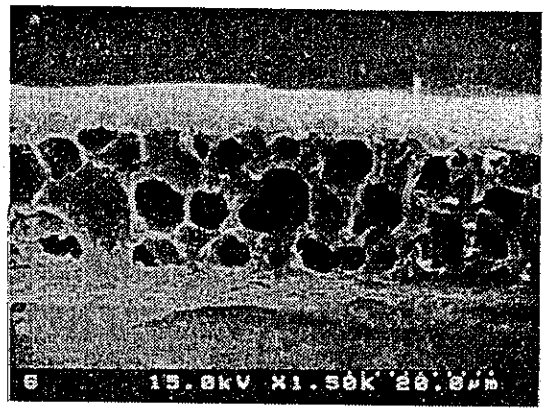

(c) 210 °C → 115 °C

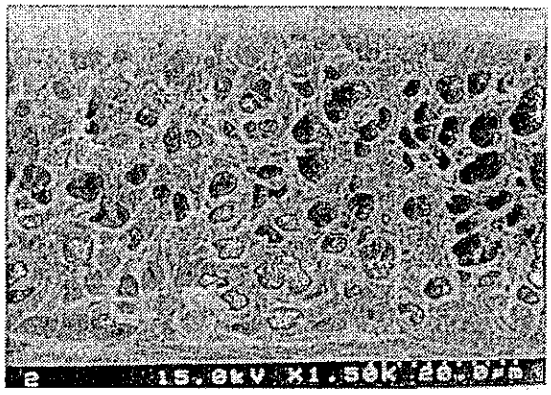

(b) 210 °C → 105 °C

iPP/DPE = 10/90 wt% sample

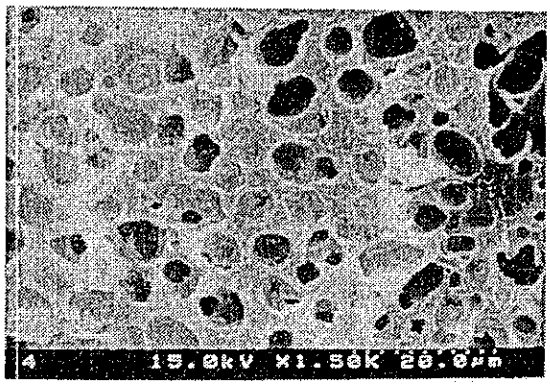

(d) 210 °C → 105 °C

iPP/DPE = 20/80 wt% sample

Figure 15. SEM images of membranes prepared from different PP/DPE compositions.

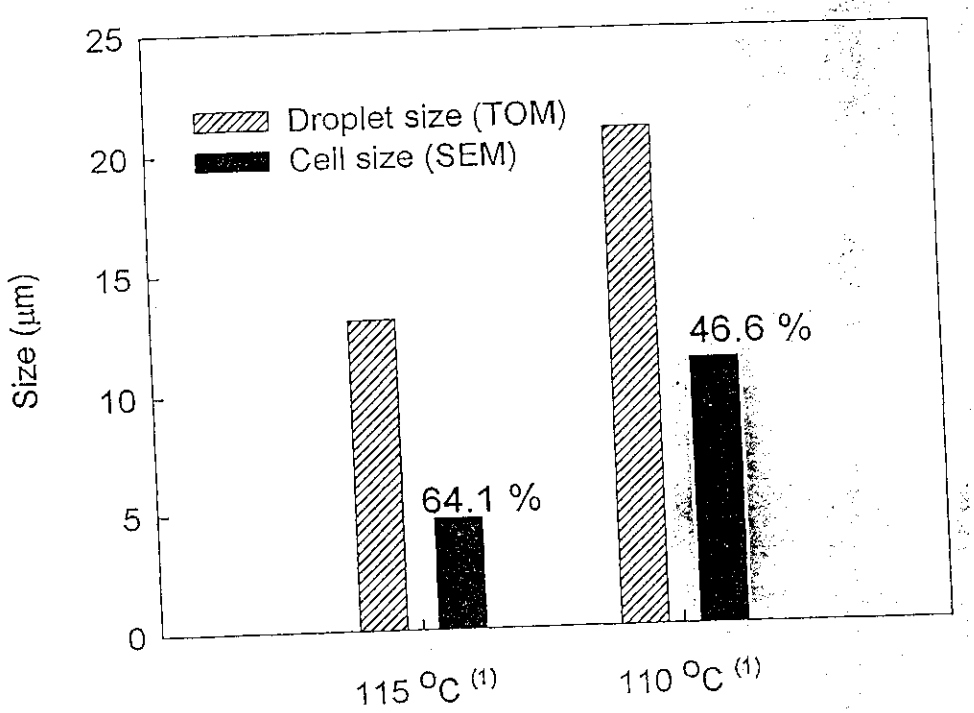

Figure 16. Comparison of droplet and cell sizes of the sample PP/DPE=20/80 wt.% held for 10 min.

equilibrium droplet size was estimated by the Laplace equation. The estimated droplet size was in good agreement with the experimental value. The droplet growth kinetics were examined in terms of the equation proposed by Furukawa. κ increased as quench temperature decreased, and λ increased with an increase of PP content. For a 10 wt.% PP sample, λ increased as the quench temperature decreased. For a 20 wt.% PP sample, λ was essentially constant (~0.3) for all quench temperatures, as previously proposed by Furukawa. The cell size in the membrane was about half of the droplet size because of shrinkage induced by extraction of the diluent and the subsequent drying process.

Acknowledgements

The authors gratefully acknowledge the financial support of Korea Science and Engineering Foundation (#961-0803-025-2 and #97K3-1005-02-09-3).

Literature Cited

1. Howell, J.A.; Sanchez, V.; Field, R.W. *Membranes in Bioprocessing*; Chapman & Hall: London, 1993.
2. Degen, P.J.; Lee, J. *U.S. Patent 5,492,781* (1996).
3. Kesting, R. E. *Synthetic Polymeric Membranes;* John Wiley & Sons: New York, 1985.
4. Kim, S.S.; Lloyd, D.R. *J. Membrane Sci.* **1991**, *64*, 13.
5. Cahn, J.W. *ACTA Metallurgica* **1961**, *9*, 795.
6. Smolders, C.A.; van Aartsen, J.J.; Steenbergen, A. *Kolloid-Z. u. Z. Polymere* **1971**, *243*, 14.
7. Song, S.W.; Torkelson, J.M. *Macromolecules* **1994**, *27*, 6389.
8. Tsai, F.J.; Torkelson, J.M. *Macromolecules* **1990**, *23*, 775.
9. Nojima, S.; Shiroshita K.; Nose T. *Polymer J.* **1982**, *14*, 289.
10. Kim, S.S.; Lloyd, D.R.; Kinzer, K.E. *J. Membrane Sci.* **1991**, *64*, 1.
11. Lloyd, D.R.; Kinzer, K.E.; Tseng, H.S. *J. Membrane. Sci.***1990**, 52, 239.
12. McGuire, K.; Laxminarayan, A.; Lloyd, D.R. *Polymer* **1995**, *36*, 4951.
13. McGuire, K.; Laxminarayan, A.; Martula, D.S.; Lloyd, D.R. *J. Colloid & Interface Sci.* **1996**, *182*, 46.
14. Laxminarayan, A. Ph.D. Dissertation, The University of Texas at Austin, 1994.
15. Laxminarayan, A.; McGuire, K.S.; Kim, S.S.; Lloyd, D.R. *Polymer* **1994**, *35*, 3060.
16. Andreas, J.M.; Hauser, E.A.; Tucker, W.B. *J. Phys. Chem.* **1938**, *42*, 1001.
17. Lee, H.K.; Myerson, A.S.; Levon, K. *Macromolecules* **1992**, *25*, 4002.
18. Zryd, I.L.; Burghardt, W.R. *J. Appl. Polym. Sci.***1995**, *57*, 1525.

19. McGuire, K.S.; Lloyd, D.R.; Lim, G.B.A. *J. Membrane. Sci.* **1993**, *79*, 27.
20. Wang, Y.F.; Lloyd, D.R. *Polymer* **1993**, *34*, 2324.
21. Wang, Y.F.; Lloyd, D.R. *Polymer* **1993**, *34*, 4740.
22. Cha, B.J.; Char, K.; Kim, J.-J.; Kim, S.S.; Kim, C.K. *J. Membrane Sci.* **1995**, *108*, 219.
23. Miller, C.M.; Neogi, P. *Interfacial Phenomena;* Marcel Dekker, Inc., New York, 1985; pp 1-44.
24. *CRC Handbook of Chemistry and Physics, 75th Ed.;* Lide, D.R. Ed.; CRC Press, Boca Raton, 1995.
25. Adamson, A. W. *Physical Chemistry of Surfaces, 5th Ed;* Wiley-Interscience: New York, 1990.
26. Van Krevelen, D.W. *Properties of Polymers, 2nd Ed.*; Elsevier, Amsterdam, 1976.
27. Lifshitz, I.M.; Slyozov, V.V. *J. Phys. Chem. Solids* **1961**, *19*, 35.
28. Siggia, E. D. *Phys. Rev.* **1979**, *A20*, 59.
29. Binder, K.; Stauffer, D. *Phys. Rev. Lett.* **1974**, *33*, 1006.
30. Wong, N.C.; Knobler, C.M. *J. Chem. Phys.* **1978**, 69, 725.
31. Chou, Y.C.; Goldburg, W.I. *Phys. Rev.* **1979**, *A20*, 2105.
32. Furukawa, H. *Adv. Phys.* **1985**, *34*, 703.